Three Classes of Motion in the Dynamic Neutron-Scattering Susceptibility of a Globular Protein

Liang Hong, Nikolai Smolin, Benjamin Lindner, Alexei P. Sokolov, and Jeremy C. Smith

Phys. Rev. Lett. **107**, 148102 — Published 30 September 2011

DOI: 10.1103/PhysRevLett.107.148102

Three classes of motion in the dynamic neutron scattering susceptibility of a globular protein

Liang Hong,[1] Nikolai Smolin,[1] Benjamin Lindner, [1] Alexei P. Sokolov,[2,3] and Jeremy C. Smith[1,*]

[1]*University of Tennessee/Oak Ridge National Laboratory Center for Molecular Biophysics, P.O.Box 2008, Oak Ridge TN 37831-6164, USA.*

[2]*Department of Chemistry, University of Tennessee, 1420 Circle Drive, Knoxville, TN 37996, USA*

[3]*Chemical Sciences Division, Oak Ridge National Laboratory, Oak Ridge, TN 37831, USA*

Abstract

A simplified description of the 295K dynamics of a globular protein over a wide frequency range (1 to 1000 GHz) is obtained by combining neutron scattering of lysozyme with molecular dynamics (MD) simulation. The MD agrees quantitatively with experiment for both the protein and the hydration water and shows that, whereas the hydration water molecules sub-diffuse, the protein atoms undergo confined motion decomposable into three distinct classes: localized diffusion, methyl group rotations and jumps. Each of the three classes gives rise to a characteristic neutron susceptibility signal.

PACS: 87.15.H-, 87.15.ap, 87.64.Bx, 87.14.E-

*Author to whom correspondence should be addressed: smithjc@ornl.gov

The dynamics of globular proteins and associated hydration water is critical to folding and function [1-6]. Much research has centered on the *ps* to *ns* timescales. However, on these timescales proteins exhibit a wide variety of diffusive and vibrational dynamics [1,7,8], and this variety has rendered difficult the derivation of a simplified description of protein internal motions in terms of a small number of distinct, superposable components. In this letter we combine neutron scattering with molecular dynamics (MD) simulation to obtain this decomposition.

Neutron scattering is a particularly useful technique for probing atomic motions in proteins, as neutrons directly probe fluctuations in nuclear positions. Consequently, a large body of research exists on the application of this technique to proteins [e.g., 3,7-15]. MD is complementary to neutron scattering, and provides, in principle, a complete description of atomic dynamics, but requires the experiment for validation. In the present work on hydrated lysozyme, excellent, quantitative agreement between neutron experiment and simulation is seen. The analysis clearly shows that on the *ps* to *ns* time scales whereas the hydration water exhibits sub-diffusive motions, the protein motions are confined. Most importantly, we demonstrate that the neutron susceptibility signal of protein can be decomposed into contributions from three distinct classes of confined motions: methyl group rotations, localized diffusion and non-methyl jumps.

Details of the experiments are given in Refs. [8,15] and of the simulation system and MD protocol in Supplemental Material [16]. The simulation box, replicated with periodic boundary conditions, contained two randomly-oriented lysozyme molecules (1AKI [17]) hydrated to h=0.3 g water / g protein, equivalent to approximately

monolayer coverage [12], and neutralized by 16 chloride ions. The incoherent intermediate scattering function, *I(q,t)*, is given by,

$$I(\vec{q},t) = \frac{1}{Z}\sum_{j}^{Z} b_j{}^2 \left\langle \exp[-i\vec{q}\vec{R}_j(0)]\exp[i\vec{q}\vec{R}_j(t)] \right\rangle, \quad (1)$$

where $\vec{q}$ is the scattering wavevector, Z is the total number of the hydrogen atoms, b_j is the incoherent scattering length of a given atom j, $\vec{R}_j$ is the position vector of that atom and the brackets denote an average over the time origin. *I(q,t)* and its time Fourier transform, the dynamic structure factor, *S(q, ν)*, were computed from the MD trajectories using in-house software. Details can be found in Ref. [16]. Only non-exchangeable hydrogen atoms, which make up about half the atoms in the protein and are relatively uniformly distributed, are concerned in the calculation of the neutron scattering spectra of protein, as they dominate the incoherent scattering signal.

It is informative to present the neutron scattering spectra as the imaginary part of the dynamic susceptibility, $\chi''(q,\nu) \propto \frac{S(q,\nu)}{n_B(\nu)}$, where $n_B(\nu)$ is the Bose occupation number $n_B(\nu)=(\exp(h\nu/kT)-1)^{-1}$. Whereas relaxation processes on different time scales are usually hard to identify in *S(q, ν)*, they appear as distinct peaks in χ'' with associated relaxation times $\tau = 1/2\pi\nu$ [8].

The susceptibility spectrum of the protein calculated from the simulation agrees well over a broad frequency range with the corresponding experimental data [8,15], obtained on lysozyme in D_2O at the same hydration level and temperature (295K)

(Fig.1a). The low-frequency peak between 0.5 to 100 GHz (~ 0.02 to 4 cm^{-1}) has been named the "main relaxation peak" [15] and we retain this terminology. The peak was fitted by a Cole-Cole distribution function [18]:

$$\chi''(\nu) = \chi_0 \frac{(\nu/\nu_{\max})^{1-\alpha}\cos(\frac{\pi\alpha}{2})}{1+2(\nu/\nu_{\max})^{1-\alpha}\sin(\frac{\pi\alpha}{2})+(\nu/\nu_{\max})^{2-2\alpha}}, \quad (2)$$

where ν_{max}, α and χ_0 are fitting parameters. Eq. (2) is traditionally used to describe symmetrically stretched relaxation peaks, as have been observed frequently in biological systems, see *e.g.,* Refs. [15,18].

Fitting Eq. (2) to χ'' at different wave vectors, q revealed that, within error, the relaxation time is independent of q in the range 0.4 to 1.6 $Å^{-1}$ (Fig. 2s in Ref. [16]), consistent with neutron scattering data on hydrogenated lysozyme in D_2O [8]. This q-independent behavior indicates that the protein atoms undergo motion confined within a radius of ~3.5Å (~$2\pi/q_{\max}$) [8].

In contrast to the protein, the dynamics of the hydration water exhibits strongly q-dependent characteristic relaxation time, τ that can be approximated by a power law (Fig. 1b): $\tau \propto q^{-n}$ with n≈2.5. This power law agrees well with corresponding experimental data for hydration water obtained from neutron scattering on fully deuterated phycocyanin hydrated with H_2O [14]. A linear fit to the experimental data yielded an exponent of n = 2.44 [14], close to the above simulation-derived value. A power law dependence of τ with the exponent n > 2 usually indicates sub-diffusion [14,19] and is often observed in glass-forming liquids [19]. In contrast, for classical Brownian diffusion

n = 2 [19,20], and this was indeed found here in a bulk water simulation with the same water model.

We now focus on the microscopic details of the confined motion that leads to the main relaxation peak of the protein (Fig. 1a). Experimental neutron scattering spectra have been described using a variety of analytical models, e.g., jumps, rotation and localized diffusion in a sphere [8,10,11]. However, due to the large variety of *ps-ns* relaxation processes in proteins [1,8,10,11,13], direct decomposition without MD simulation of ensemble-averaged experimental neutron scattering data into contributions from distinct processes is very challenging and does not provide an unambiguous determination of the microscopic nature of the atomic motions involved [8].

To perform the decomposition, the coordinates of each hydrogen atom at every 1 *ps* in a 10 *ns* MD trajectory were projected onto scatter plots. Typical examples of scatter plots are presented in Figs. 2a-d and videos of simulated atomic motions corresponding to Figs. 2a-d are provided in Ref. [16]. Visual examination of the scatter plots reveals two types of hydrogen atom: (I) diffusing inside a single localized region (Fig. 2a), which we denote as a "cluster", and (II) diffusing in clusters and occasionally jumping between them (Figs. 2b-d). About 60% of the non-exchangeable hydrogen atoms were found to belong to Type I.

Methyl hydrogen atoms perform 3-fold rotational jumps (e.g., Fig. 2c). Experimental work has provided indirect evidence that methyl group rotations contribute significantly to neutron scattering spectra on the *ps* to *ns* time scales [8,11,13]. Moreover, the temperature dependence of the methyl rotations follows an Arrhenius law [21,22], unlike other protein motions in the same time window [15]. Therefore, it is useful to

separate the methyl group rotations from the other jumps. Hence, in what follows, we categorize the motions of the protein hydrogen atoms in three classes: "localized diffusion", "methyl group rotations" and "jumps excluding methyl group rotations" (which we call, for simplicity, "jumps"), and analyze them separately. The classification of atomic motions proposed here should not be confused with the classification of hydrogen atoms made above. A Type I hydrogen atom performs only "localized diffusion" (Fig. 2a), while a Type II hydrogen atom conducts both "localized diffusion" and also "methyl group rotations" (Fig. 2c) and/or "jumps" (Figs. 2b and d).

In order to obtain the neutron scattering spectrum arising solely from the methyl group rotations the susceptibility spectrum, χ''_{nome} was computed of the trajectory in which the 3-fold methyl group rotations were removed (details can be found in Ref. [16]). Thus, the scattering component coming from methyl group rotations can be estimated as $\chi''_{me} = \chi'' - \chi''_{nome}$, where χ'' is the total spectrum. To obtain the neutron scattering spectrum resulting from only the (non methyl rotation) jumps, it is necessary to subtract from the total spectrum the contributions from the localized diffusion of all the hydrogen atoms (both Type I and II) and from the methyl group rotations. With the assumption that the scattering signal arising from the localized diffusion of Type I and Type II hydrogen atoms are the same, the spectrum of "jumps" is given by $\chi''_{jump} \cong \chi'' - \chi''_{me} - \chi''_{ld} \cong \chi'' - \chi''_{me} - \frac{N_{non-ex}}{N_{Type-I}} \chi''_{Type-I}$, where the subscript "*ld*" denotes "localized diffusion summed over Type I and II hydrogen atoms", $N_{non\text{-}ex}$ (=1392) and $N_{Type\text{-}I}$ (=796) are the numbers of non-exchangeable and Type I protein hydrogen atoms in

the simulation primary box, and $\chi''_{Type\text{-}I}$ is the susceptibility spectrum of the Type I hydrogen atoms.

Fig. 3a shows that the protein χ''over the 1 to 100 GHz frequency window can be decomposed into three components: the localized diffusion, the methyl group rotations and the jumps. We now examine each of these components.

Fig. 3b presents the time dependence of the mean-square displacement, $<x^2>$, of a typical example of the localized diffusion of a Type I hydrogen atom, which exhibits two plateaux. The fast increase in $<x^2>$ at 0.1-0.3*ps,* which is followed by the first plateau at times up to ~3*ps*, reflects the "fast relaxation" process [7,23], *i.e.,* rattling of the atom inside the cage formed by neighbors [23], or arises from dephasing of the vibrational modes [24]. At longer times (t >3 *ps*), $<x^2>$ departs from the cage region, and eventually reaches a second plateau at ~200 *ps*, corresponding to diffusion within the cluster. This second plateau originates from the cluster-size confinement, and the square root of $<x^2>$ at this plateau is 0.7Å, in accord with the ~0.9Å radius of the cluster in Fig. 2a. Statistical analyses of the cluster geometry of Type I hydrogen atoms were performed and are reported in Ref. [16]. The distribution of the radius of gyration, R_g, of the clusters is broad, ranging from 0.3 to 1.4Å with a maximum around 0.5Å (Fig. 4s in Ref. [16]). Also, the asphericity parameters are low, indicating that the volumes in which they diffuse are close to spherical (Fig. 4s in Ref. [16]). As shown in Fig. 3a, the susceptibility spectrum of the localized diffusion (χ''_{ld}) is quite flat in the frequency window ~1-100 *GHz*, consistent with the broad cluster-size distribution.

The contribution of the methyl group rotations (χ''_{me}) to the main relaxation peak in Fig. 3a is larger than either of the other two components and possesses a noticeable peak located around 10 GHz, symmetrically stretched on both the low- and high-frequency sides. The symmetrical stretching makes Eq. (2) an appropriate function to fit this peak, yielding an average relaxation time $\bar{\tau}_{methyl}$ =22 *ps*. The rotation of the methyl groups usually follows an Arrhenius temperature dependence, $\tau=\tau_0\exp(\Delta E/kT)$, with $\tau_0 \sim$ 0.18 *ps* [21,22]. Accordingly, $\bar{\tau}_{methyl}$ estimated above would correspond to an average rotational barrier: ΔE = 2.8 kcal/mol, which is consistent with the experimental values of ~ 3 kcal/mol obtained in a variety of studies [8,11,21,22].

χ''_{jump} exists mainly below 10 GHz (Fig. 3a), and the associated relaxation peak is thus out of the frequency range studied here. Hence, the corresponding average relaxation time will be several *ns* or longer and may correspond to the 'slow' process recently discussed in Ref. [25]. If this is correct, our analysis provides the first microscopic picture of the motion involved.

Characterization of the temperature and hydration dependence of the dynamics of wet protein powders using the present approach will be of particular interest. Methyl group rotation is activated in proteins from ~100K upwards and is hydration-independent [8,11,13]. At higher temperatures (180 ~ 220 K) a further, hydration-dependent transition occurs [8,9,11-13], during which there is simulation evidence that jumps between minima are activated [26].

Using the present protein and solvent force fields Figs. 1 show that MD simulations reproduce the neutron scattering susceptibility of the protein quantitatively

over a wide frequency range (1 to 1000GHz). Whereas a single MD simulation is sufficient to obtain the spectrum over this wide frequency range, the corresponding experiment requires considerable effort, involving the combination of several instruments [8,15,18]. The analysis shows that, at low hydration, the water undergoes sub-diffusive motion, while the protein atoms perform confined motions that can be decomposed into three classes: localized diffusion, methyl rotation and jumps. As these three types of atomic motion occur on similar time and length scales, they would have been difficult to identify and tease apart *a priori* by directly fitting simple analytical models to the ensemble-averaged experimental neutron scattering data [8,10,11,13]. The present results demonstrate how MD can provide a model-free interpretation of the spectra in terms of a simple decomposition of the hydrogen-atom fluctuations in a globular protein.

Acknowledgment

The authors thank Dr. E. Mamontov's help for analyzing the BASIS data and acknowledge DOE support through EPSCoR program (grant DE-FG02-08ER46528).

References

[1] H. Frauenfelder, S. G. Sligar, and P. G. Wolynes, Science **254**, 1598 (1991).

[2] C. D. Snow *et al*., Nature **420**, 102 (2002).

[3] R. Biehl *et al*., Phys. Rev. Lett. **101**, 138102 (2008).

[4] L. Zhu, D. Frenkel, and P. G. Bolhuis, Phys. Rev. Lett. **106**, 168103 (2011).

[5] J. Pieper *et al*., Phys. Rev. Lett. **100**, 228103 (2008).

[6] F. Piazza, P. DeLosRios, and F. Cecconi, Phys. Rev. Lett. **102**, 218104 (2009).

[7] W. Doster, S. Cusack, and W. Petry, Phys. Rev. Lett. **65**, 1080 (1990).

[8] J. H. Roh *et al*., Biophys. J. **91**, 2573 (2006).

[9] G. Zaccai, Science **288**, 1604 (2000).

[10] J. Fitter *et al*., Proc. Natl. Acad. Sci. USA. **93**, 7600 (1996).

[11] J. H. Roh *et al*., Phys. Rev. Lett. **95**, 038101 (2005).

[12] S. H. Chen *et al*., Proc. Natl. Acad. Sci. USA **103**, 9012 (2006).

[13] W. Doster, Biochim. Biophys. Act. **173**, 1749 (2005).

[14] S. Dellerue and M. -C. Bellissent-Funel, Chem. Phys. **258**, 315 (2000).

[15] S. Khodadadi *et al*., J. Chem. Phys. **128**, 195106 (2008).

[16] Supplemental Material.

[17] P. J. Artymiuk *et al*., Acta Crystallogr., Sect. B **38**, 778 (1982).

[18] S. Khodadadi *et al*., Biophys. J. **98**, 1321 (2010).

[19] J. Colmenero *et al*., Phys. Rev. Lett. **69**, 478 (1992).

[20] F. Volino and J. Dianoux, Mol. Phys. **41**, 271 (1980).

[21] B. Frick and L. J. Fetters, Macromolecules **27**, 974 (1994).

[22] Y. Xue *et al*., J. Am. Chem. Soc. **129**, 6827 (2007).

[23] W. Gotze and L. Sjogren, Rep. Prog. Phys. **55**, 241 (1992).

[24] J. C. Smith *et al*., J. Chem. Phys. **93**, 2974 (1990).

[25] S. Khodadadi, J. E. Curtis, and A.P. Sokolov, J. Phys. Chem. B **115**, 6222 (2011).

[26] A. L. Tournier and J. C. Smith, Phys. Rev. Lett. **91**, 208106 (2003).

Figure Captions

Fig. 1 (color online). (a) Susceptibility spectra of hydrated lysozyme (q = 1 Å^{-1}) obtained from neutron scattering experiments on the NIST high-flux backscattering spectrometer (HFBS, triangles), the ORNL SNS back-scattering spectrometer (BASIS, spheres), the NIST disk-chopper time-of-flight spectrometer (TOF, squares) [8,15] and from MD simulation (thick solid line). To improve the statistics, the experimental spectra were summed over the q range from 0.3 to 1.7 Å^{-1} with an average q = 1 Å^{-1}. The experimental data on the y axis were multiplied by an arbitrary constant for ease of comparison of the shape of the two spectra. Experimental intensity is difficult to obtain on an absolute scale, and even more so when combining several instruments. Hence, only the shape of the spectra can be compared. (b) q dependence of the average main relaxation time (τ) of water molecules presented on a double logarithmic scale. Simulation results are denoted as empty symbols: hydration water (squares) and bulk water (spheres). The solid squares are experimental data for hydration water [14]. The dashed lines are linear fits to the simulation data yielding slopes of 2.5 for the hydration water and 2.0 for the bulk. The susceptibility spectra of hydration and bulk water at different q values, from which τ is estimated, are presented in Fig. 3s in Ref. [16].

Fig. 2 (color online). Typical examples of scatter plot projections of hydrogen-atom trajectories from MD. (a): Diffusion in a single cluster (the δ hydrogen atom of TRP63).(b-d) Diffusion in clusters plus jumping between (b) two clusters (a γ hydrogen

atom of ARG150) (c) three clusters (a methyl hydrogen atom of VAL2) and (d) four clusters (a γ hydrogen atom of LYS226).

Fig. 3 (color online). (a) MD Neutron susceptibility spectrum of the whole protein (χ''), the localized diffusion (χ''_{ld}) summed over Type I and II hydrogen atoms, the methyl group rotations (χ''_{me}), and the jumps (χ''_{jump}). (b) $\langle x^2 \rangle$of the same hydrogen atom as in Fig. 2a, the ballistic region at $t < 0.1$ *ps* is not shown.

Fig. 1

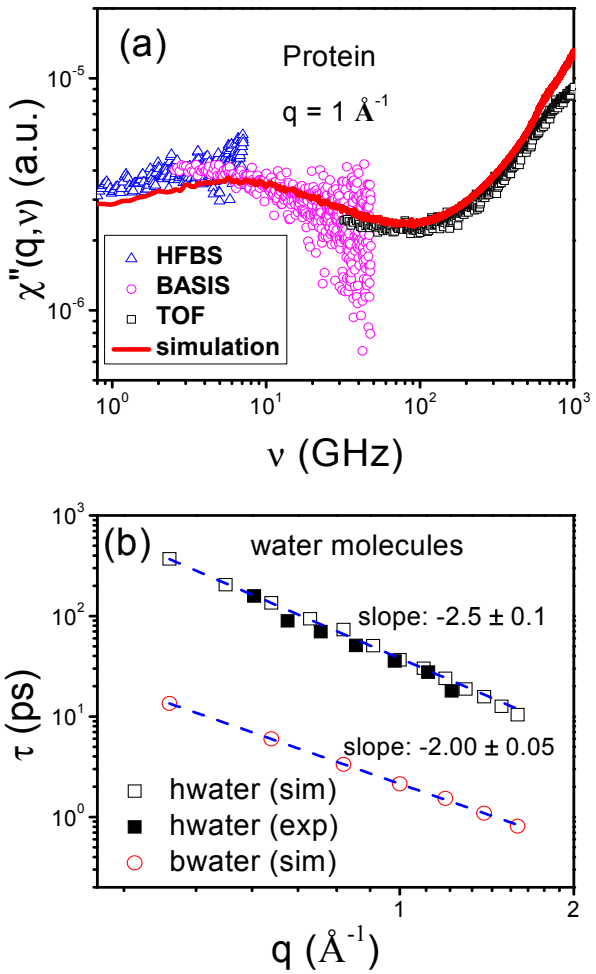
(a)
Protein
q = 1 Å^{-1}
χ"(q,ν) (a.u.)
HFBS
BASIS
TOF
simulation
ν (GHz)
(b)
water molecules
slope: -2.5 ± 0.1
slope: -2.00 ± 0.05
hwater (sim)
hwater (exp)
bwater (sim)
τ (ps)
q (Å^{-1})

Fig. 2

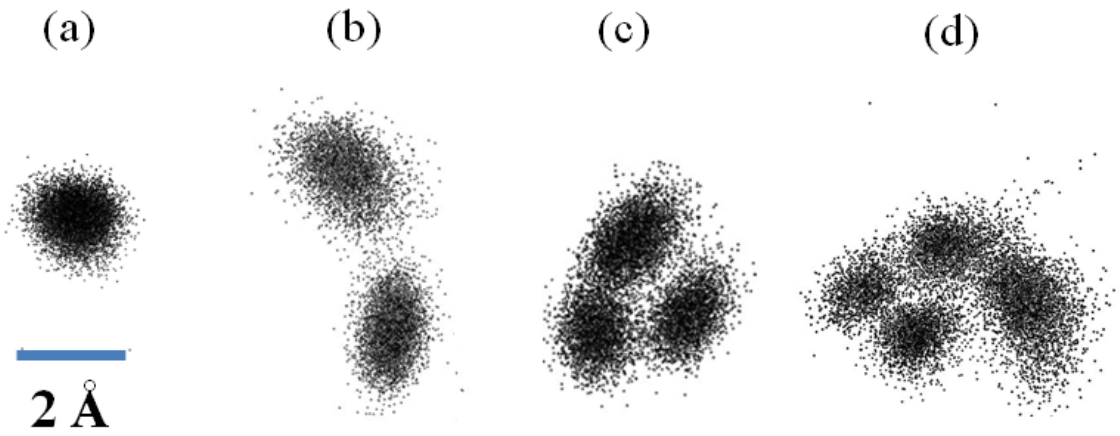

Fig. 3

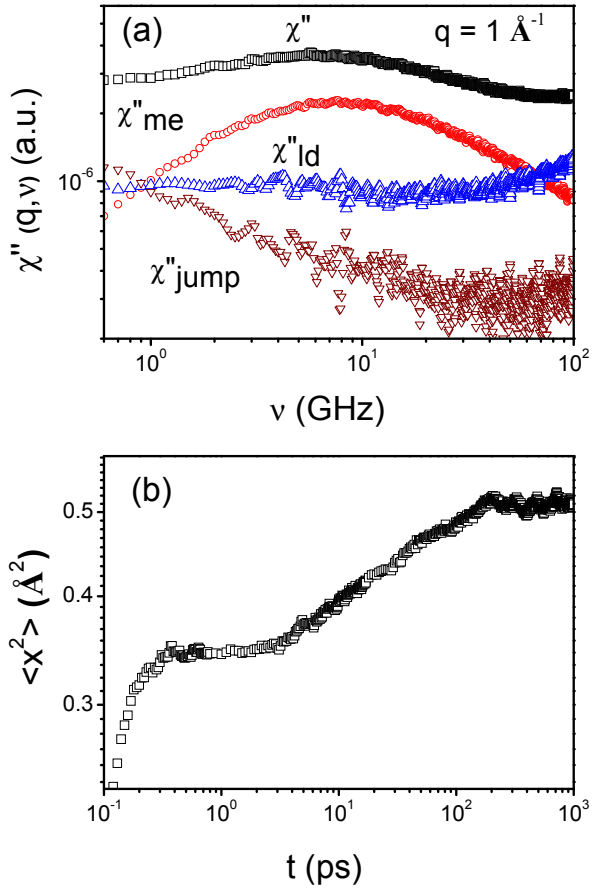
(a)
χ"
q = 1 Å-1
χ"me
χ"ld
χ"jump
10-6
χ" (q,ν) (a.u.)
10^0
10^1
10^2
ν (GHz)
(b)
0.5
0.4
0.3
<x2> (Å2)
10-1
10^0
10^1
10^2
10^3
t (ps)